RSC Advances

PAPER

View Article Online
View Journal | View Issue

Cite this: *RSC Adv.*, 2022, **12**, 24752

Up-conversion luminescence properties with temperature change of strontium tungstate phosphors

Soung-Soo Yi[a] and Jae-Yong Jung *[b]

Thermally stable $SrWO_4$:[Er^{3+}]/[Yb^{3+}] upconversion phosphors were synthesized. X-ray diffraction analysis indicated a crystalline inorganic phosphor material with a tetragonal structure having a clear peak in the (112) phase, which is the main peak. The upconversion phosphor was synthesized using a precursor prepared by co-precipitation and sintered at 800 °C. When the phosphor was excited by a 980 nm laser with a pumping power of 200 mW, a strong green light was emitted. As the concentration of Er^{3+} ions increased, it was observed that the emission intensity decreased due to concentration quenching. The changes in the intensity of luminescence according to the pumping power are due to a two-photon process. As the temperature increased, the green emission intensity of the up-conversion phosphor increased. This was thought to be a phenomenon caused by efficient energy transfer between Yb^{3+} and Er^{3+} ions by the $SrWO_4$ host with negative thermal expansion. A composite was prepared by mixing phosphor powder and PDMS, that could be used for temperature sensing.

Received 28th July 2022
Accepted 26th August 2022

DOI: 10.1039/d2ra04705e

rsc.li/rsc-advances

1 Introduction

Up-conversion phosphors are materials that emit light by fusing low-energy photons and converting them into high-energy photons, and these phosphors are attracting attention in various fields such as sunlight, bio-emerging, and phosphor applications.[1,2] Existing down-conversion phosphors are mainly based on Stokes emission, which generates low energy long wavelength visible light from high energy short wavelengths such as the ultraviolet region.[3,4] In contrast to this Stokes emission, upconversion phosphors have an anti-Stokes-emission mechanism in which long-wavelength photons fuse to produce short-wavelength photons.[5,6] By using an up-conversion phosphor, light in the infrared region can be converted into visible light, or light in the visible region can be converted into ultraviolet light.[7,8] This can be considered a phenomenon that violates the laws of thermodynamics, but the up-conversion phenomenon is possible because it is an emission phenomenon that occurs by the fusion of energy of two or more photons, not by a single photon.[9,10] Research on up-conversion phosphors has been actively conducted using inorganic materials doped with rare earth ions. Up-conversion is caused by a luminescence phenomenon, due to the double excitation of photons in inorganic materials with a long lifetime transition energy region.[11,12] By absorbing the primary photon, the excited electron with the transition energy band absorbs an additional photon before falling to the ground state and is excited to a higher energy level.[13,14] Pavani *et al.* synthesized $SrLaAl_3O_7$ co-doped with Er^{3+} and Yb^{3+} by the facile Pechini method. The phosphor excited at 980 nm showed strong green emission by the $^4I_{13/2} \rightarrow {}^4I_{15/2}$ transition. In addition, the visible spectrum of 528, 548, and 660 nm was shown, and the up-conversion mechanism was reported.[15] Lim *et al.* synthesized a yellow-emitting phosphor when excited at 980 nm by co-doping Yb^{3+} and Ho^{3+} with $LiNaCaLa(MoO_4)_3$ quadruple molybdate as a host, by the microwave sol–gel method.[16] Deng *et al.* doped the $GaAlO_3$:Er^{3+}, Yb^{3+} phosphor with Lu^{3+} and Ga^{3+} ions by co-precipitation. Ga^{3+} is Al^{3+} and Lu^{3+} is Gd^{3+} substituted, and a change in the intensity of the up-conversion green emission according to the structural change in the host was reported.[17] Barrera *et al.* synthesized an up-conversion phosphor by doping Er^{3+} and Yb^{3+} ions into a $KY(WO_4)_2$ host using the Pechini method. The phosphor excited at 980 nm showed emission spectra of 530, 550, and 660 nm. A change in emission intensity according to the change in the concentration of doped rare earth ions, and a change in the intensity of the excitation light, were observed.[18] Pandey *et al.* prepared Y_2O_3 up-conversion phosphors co-doped with Ho^{3+} and Yb^{3+} ions by the combustion route. When excited with a 980 nm diode laser, the color changed according to the doping concentration of Ho^{3+} ions, as shown in the CIE color coordinates, and a visible light spectrum of strong green and relatively weak red and blue was observed.[19] Various synthesis methods and doping with rare earth ions have been performed to synthesize upconverted

[a]*Division of Materials Science and Engineering, Silla University, Busan 46958, Republic of Korea*

[b]*Research and Business Development Foundation, Silla University, Engineering Building, Busan 45985, Republic of Korea. E-mail: eayoung21@naver.com; Tel: +82-51-999-6441*

phosphors and to investigate their luminescence properties. In this study, phosphors were synthesized by co-doping with Er^{3+} and Yb^{3+} rare earth (RE) ions using strontium tungstate ($SrWO_4$), which has chemical and thermal stability, as a host. The precursor was prepared by co-precipitation and heat-treated at 800 °C. Changes in the crystal structure and luminescence characteristics of the synthesized phosphor after doping with rare earth ions were investigated. In addition, a change in luminescence characteristics according to the power and temperature of the excitation light was observed, and it was suggested that the composite could be used for temperature sensing.

2 Experimental

2.1. Synthesis of $SrWO_4$:[Er^{3+}]/[Yb^{3+}] by co-precipitation and sintering

Starting materials. Barium acetate ($(CH_3CO_2)_2Sr$, Sigma-Aldrich), sodium tungstate ($Na_2WO_4 \cdot 2H_2O$, Sigma-Aldrich), ytterbium(III) nitrate pentahydrate ($Yb(NO_3)_3 \cdot 5H_2O$, Yb^{3+}), and erbium(III) nitrate pentahydrate ($Er(NO_3)_3 \cdot 5H_2O$, Er^{3+}). 10 mmol of $(CH_3CO_2)_2Sr$ was dissolved in beaker "A" containing 100 ml of distilled water. In beaker "B", 10 mmol of $Na_2WO_4 \cdot 2H_2O$ was dissolved in 100 ml distilled water (Fig. 1). The solution that was completely dissolved in beaker "B" was slowly poured into a stirring beaker "A" and remained there for about 20 minutes. After that, powder was recovered using a centrifuge (4000 rpm, 5 min), and the powder was prepared by rinsing with distilled water 3 times to remove any remaining sodium. The powder was dried in an oven at 80 °C for 16 hours. The up-conversion phosphor was synthesized with $SrWO_4$ as a host, the precursor made by simultaneously adding $Yb(NO_3)_3 \cdot 5H_2O$ and $Er(NO_3)_3 \cdot 5H_2O$ to beaker "A". The prepared precursor was sintered at 800 °C until the $SrWO_4$:[Er^{3+}]/[Yb^{3+}] phosphor was synthesized. Rare earth [RE] ions of Yb^{3+} were fixed at 0.5 mmol, and the amount of Er^{3+} (0.05, 0.1, 0.15, 0.2, 0.25, 0.3, 0.4, 0.5 mmol) added changed ([Er^{3+}]/[Yb^{3+}] ~ 0.1, 0.2, 0.3, 0.4, 0.6, 0.8, 1).[20,21]

2.2. Characterization

The crystal structure of the synthesized phosphor powder was measured using an X-ray diffraction apparatus (XRD, X'Pert PRO MPD, 40 kV, 30 mA) having Cu-Kα radiation (wavelength: 1.5406 Å) at a scan rate of 4° min^{-1} at a diffraction angle of 10° to 70°. The size and microscopic surface shape of the crystal grains were photographed with a field emission scanning electron microscope (FE-SEM, CZ, MIRA I LMH, TESCAN). To measure the fluorescence spectrum by up-conversion, a semiconductor pulse laser (TCLDM9, Thorlabs) that emitted an output of 200 mW at a wavelength of 980 nm as excitation, and a spectrometer (HR4000, Ocean Optics) with a photomultiplier connected were used to measure the emission spectrum. To analyze the fluorescence mechanism by up-conversion, the energy absorption and energy transfer processes in the excited state were analyzed by changing the intensity of the pulsed laser and measuring the changes in the intensity of the fluorescence.

2.3. Fabrication of a temperature sensing composite

The synthesized $SrWO_4$:[Er^{3+}]/[Yb^{3+}] up-conversion phosphors were mixed with 0.1 g each and 1 g of polydimethylsiloxane (PDMS) and cast in a square mold. After curing in an oven at 80 °C for 2 hours, the prepared composite was placed on a hot plate, excited at 980 nm, and the change in luminescence intensity according to temperature change was photographed.

3 Results & discussion

3.1. Structure and morphology of $SrWO_4$:[Er^{3+}]/[Yb^{3+}] up-conversion phosphors

Fig. 2(a) shows the XRD patterns of the samples prepared by co-precipitation at room temperature and calcined at 800 °C. The synthesized $SrWO_4$ was consistent with the ICDD card no. 01-089-2568, and the tetragonal structure ($a = 5.40$ Å, $b = 5.40$ Å, $c = 11.91$ Å, space group $I4_1/a$) could be confirmed. A strong peak at 27.65° was detected, which was the (112) phase, the main peak of $SrWO_4$. In addition, the phases (101), (004), (200), (211), (204), (220), (116), (312), (224), (008), and (440) were also observed. In the $SrWO_4$:[Er^{3+}]/[Yb^{3+}] samples doped with rare earth ions for synthesis as up-conversion phosphors, the main peak (112) phase was also clearly observed. As the amount of rare earth ions increased (Er^{3+}), the detection position of the main peak (112) phase shifted, but no secondary phase was found. Using the change in the detection position of the main peak-in (112), the change in the lattice constant was calculated by substituting it into the Bragg's equation ($2d \sin\theta = n\lambda$)[22] and is shown in Fig. 2(b). The lattice constant of pure $SrWO_4$ was calculated to be 0.2901 nm, and the lattice constant decreased as the added amount of Er^{3+} ions increased ($SrWO_4$: 0.2901 nm, $SrWO_4$:[Er^{3+}]/[Yb^{3+}] ~ 0.1 : 0.2898 nm $SrWO_4$:[Er^{3+}]/[Yb^{3+}] ~ 0.4 : 0.2896 nm). Although this is a small change, due to the change in the lattice constant it means that rare earth ions were doped in the lattice. Ortega *et al.* observed a shift of 2 theta angles on (111), the main peak of CeO_2. It was reported that this was due to doping with rare earth ions having a large ionic radius ($Ce^{4+} = 0.97$ Å, $Eu^{3+} = 1.066$ Å, $La^{3+} = 1.16$ Å).[23] Ortega *et al.* observed a shift of 2 theta angles on (111), the main peak of CeO_2. It was reported that this was due to doping of rare earth ions with a large ionic radius. In this study, 2 theta angles on the main peak (112) were shifted by doping rare earth ions with relatively small ionic radii, and the lattice constant was changed, due to co-doping ($Sr^{2+} = 1.18$ Å, $Yb^{3+} = 0.868$ Å, $Er^{3+} = 0.89$ Å).[24,25] Fig. 3 shows the FE-SEM image and energy dispersive X-ray spectroscopy (EDS) component analysis of the synthesized $SrWO_4$:[Er^{3+}][Yb^{3+}] sample. The sample had a shape like a dumbbell as it was spread out widely with round ends in the form of a long cylinder. It had a size of about 4.08 μm in the longitudinal direction and about 1.38 μm in the transverse direction. Ryu *et al.* observed the change in the surface shape of the particles according to the molar ratio of Sr^{2+} and WO_4^{2-} when synthesizing crystalline $SrWO_4$ by the co-precipitation method. As the value of [WO_4^{2-}]/[Sr^{2+}] increased, the rod-like shape changed to dumbbell and spherical shapes. This phenomenon was explained as a process in which the

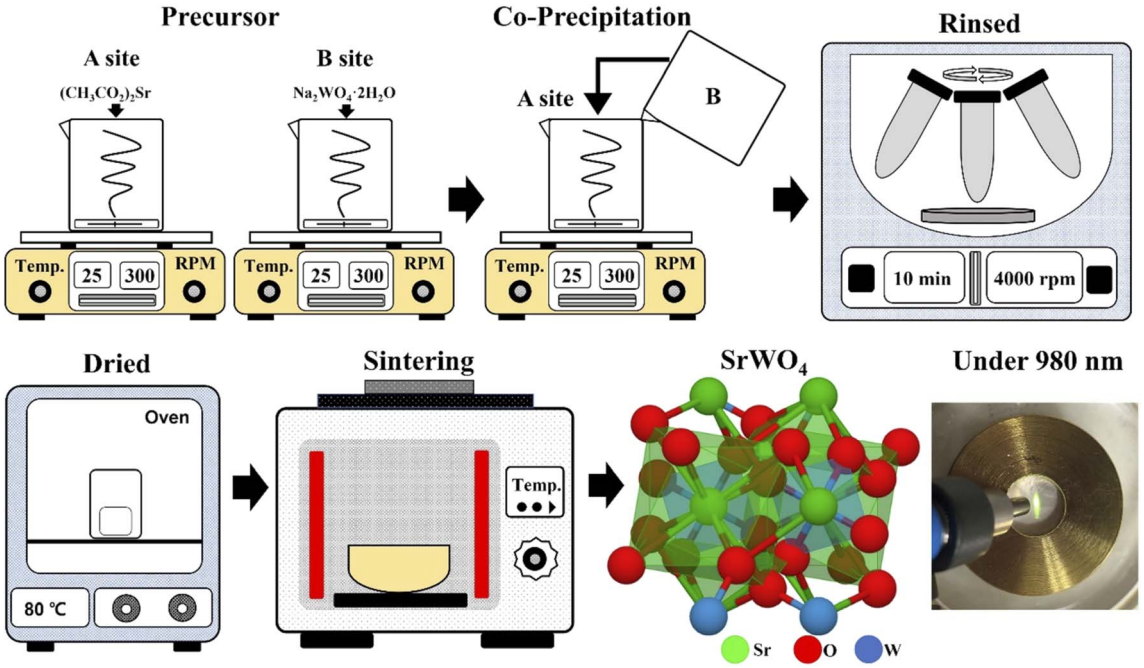

Fig. 1 Experimental procedure for preparing the $SrWO_4$:$[Er^{3+}]/[Yb^{3+}]$ up-conversion phosphors.

aggregation and growth directions of particles, *etc.*, started from both ends of the particles and eventually changed to a spherical shape due to the self-assembly reaction.[26]

3.2. Luminescence characteristics of $SrWO_4$:$[Er^{3+}]/[Yb^{3+}]$ up-conversion phosphors

Fig. 4(a) shows the photoluminescence (PL) spectrum of $SrWO_4$:$[Er^{3+}]/[Yb^{3+}]$ phosphors prepared by co-precipitation at 800 °C. When the sample was excited with a 980 nm semiconductor laser, the pump power was fixed at 200 mW. The synthesized up-conversion phosphor showed a strong green light emission signal at 520–560 nm and a relatively weak red signal spectrum at 640–680 nm. The green emission bands were centered at 529 and 543, corresponding to the ($^2H_{11/2}$, $^4S_{3/2}$) → $^4I_{15/2}$ transitions, and the red emission band was centered at 657 nm, corresponding to the $^4F_{9/2}$ → $^4I_{15/2}$ transitions of Er^{3+} ions.[27,28] It is well known that Yb^{3+} and Er^{3+} rare earth ions co-doped into a $SrWO_4$ host are absorbed by the Yb^{3+} ions of 980 nm from the outside, and then energy is transferred to the Er^{3+} ions, with emission peaks in the green and red spectrum, respectively, from the Er^{3+} ions.[29] Yb^{3+} ions are suitable co-activators because of their large absorption cross-sectional area and the high concentration at which quenching occurs, and most of the infrared energy is absorbed by Yb^{3+} ions. In Fig. 4(b), when $[Er^{3+}]/[Yb^{3+}] \sim 0.1$, the integrated area of the PL spectrum was the highest, and thus strong emissions were shown. As the concentration of Er^{3+} ions increased, PL intensity decreased, and it is considered that the energy absorbed due to the concentration quenching caused by excessive rare earth

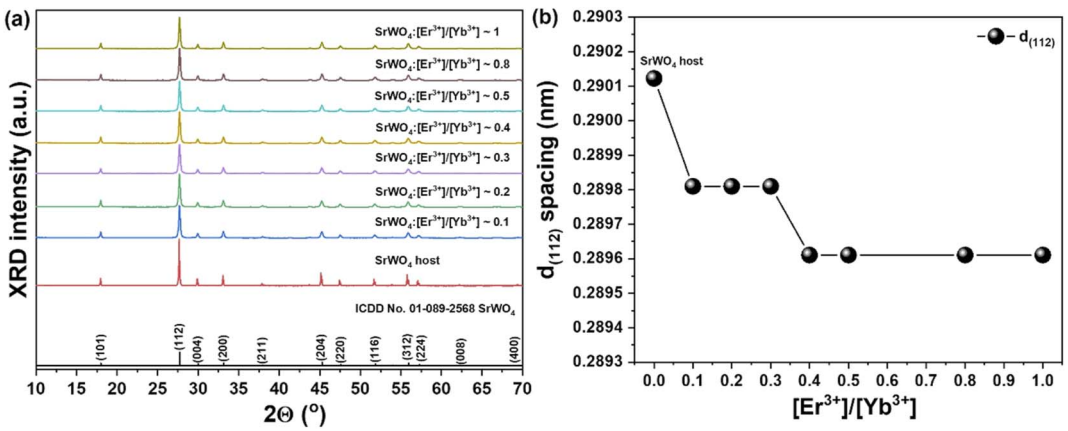

Fig. 2 (a) XRD patterns of synthesized $SrWO_4$ and $SrWO_4$:$[Er^{3+}]/[Yb^{3+}]$ powders and (b) change in $d_{(112)}$ spacing.

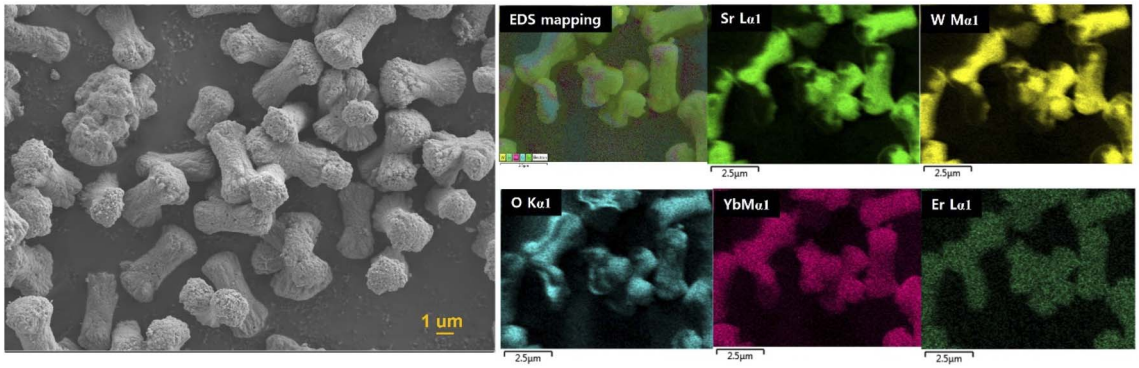

Fig. 3 FE-SEM image and EDS analysis of the $SrWO_4$:[Er^{3+}]/[Yb^{3+}] powder.

doping is caused by inefficient transfer. The [Er^{3+}]/[Yb^{3+}] ~ 0.1 sample, which showed the strongest up-conversion luminescence at a laser power of 980 nm at 200 mW, exhibited a change in up-conversion luminescence characteristics according to the change in laser power, and is shown in Fig. 5(a). The laser power was varied from 75 to 280 mW. A band of strong green emission was still observed, and the intensity of the emission spectrum also increased as the laser power increased (Fig. 5(b)). The up-conversion process induces an energy transfer (ET) process, in which energy absorbed by Yb^{3+} ions is transferred to Er^{3+} ions, and an excited state absorption (ESA) process by the transfer of additional energy to the excited Er^{3+} ions. The ESA process occurs in a single ion, while the ET process occurs when two rare earth ions are involved. The $SrWO_4$[Er^{3+}]/[Yb^{3+}] ~ 0.1 phosphor to which Er^{3+} and Yb^{3+} ions are added absorbs photons from a 980 nm laser, and Yb^{3+} ions at the $^2F_{7/2}$ level are excited to the $^2F_{5/2}$ level. The excited Yb^{3+} ions are adjacent to Er^{3+} ions, which excite the Er^{3+} ions to the $^4I_{11/2}$ level through ET ($^2F_{5/2}$ (Yb^{3+}) + $^4I_{15/2}$ (Er^{3+}) → $^2F_{7/2}$ (Yb^{3+}) + $^4I_{11/2}$ (Er^{3+})) and return to the ground state.[30–32] When an up-conversion phosphor with a wavelength of 980 nm is pumped by an excitation source, the Er^{3+} ions are excited to the $^4I_{11/2}$ level through the ET_1 process, and the GSA process, as shown in Fig. 5(c). The lifetime of the $^4I_{11/2}$ level is long enough that electrons are occupied at the $^4F_{7/2}$ level of the Er^{3+} ion by the ET_3 ($^2F_{5/2}$ (Yb^{3+}) + $^4I_{11/2}$ (Er^{3+}) → $^2F_{7/2}$ (Yb^{3+}) + $^4F_{7/2}$ (Er^{3+})) process and the ESA_1 process by the Yb^{3+} ion excited by the absorption of another photon.[33] Another way electrons can be occupied at the $^4F_{7/2}$ level is the cross-relaxation process that occurs between adjacent Er^{3+} ions. One of the two Er^{3+} ions in the $^4I_{11/2}$ level interacts with an adjacent ion to gain energy and move to $^4F_{7/2}$, and the other ion loses energy and transitions to the ground state $^4I_{15/2}$ level.[34] By this process, two green lights are emitted at a wavelength of 529 nm by the $^2H_{11/2}$ → $^4I_{15/2}$ transition and 543 nm by the $^4S_{3/2}$ → $^4I_{15/2}$ transition. In the observed red spectrum, electrons are occupied at the $^4I_{13/2}$ level by non-radiative transition from the $^4I_{11/2}$ level, and the electrons are occupied at the $^4F_{9/2}$ level through the ET_2 and ESA_2 processes. Then, red light of 657 nm is emitted by $^4F_{9/2}$ → $^4I_{15/2}$ transition.[35] The intensity of fluorescence by up-conversion is related to the fluorescence intensity of pump excitation light by the following equation:[36]

$$I \propto P^n \quad (1)$$

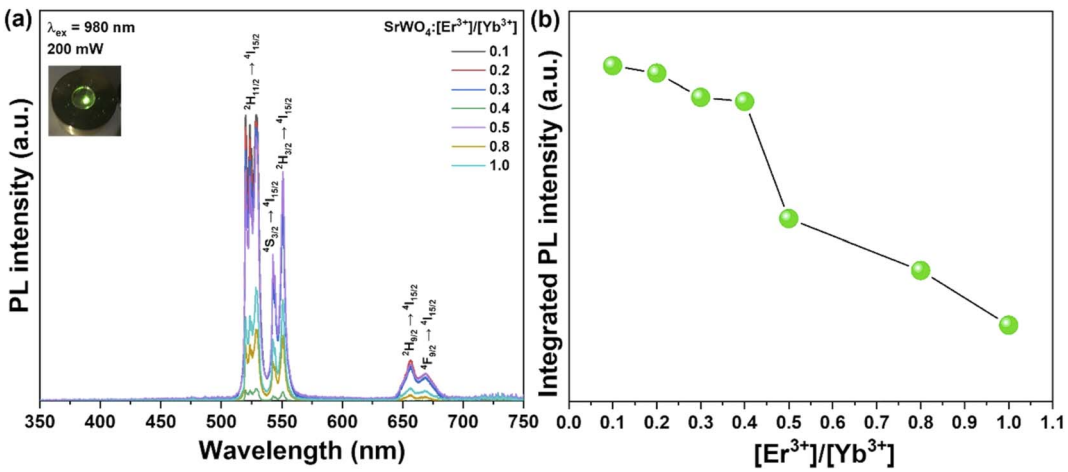

Fig. 4 (a) PL spectra under 980 nm and (b) change in PL intensity according to Er^{3+} concentration at 200 mW in the $SrWO_4$:[Er^{3+}]/[Yb^{3+}] up-conversion phosphors.

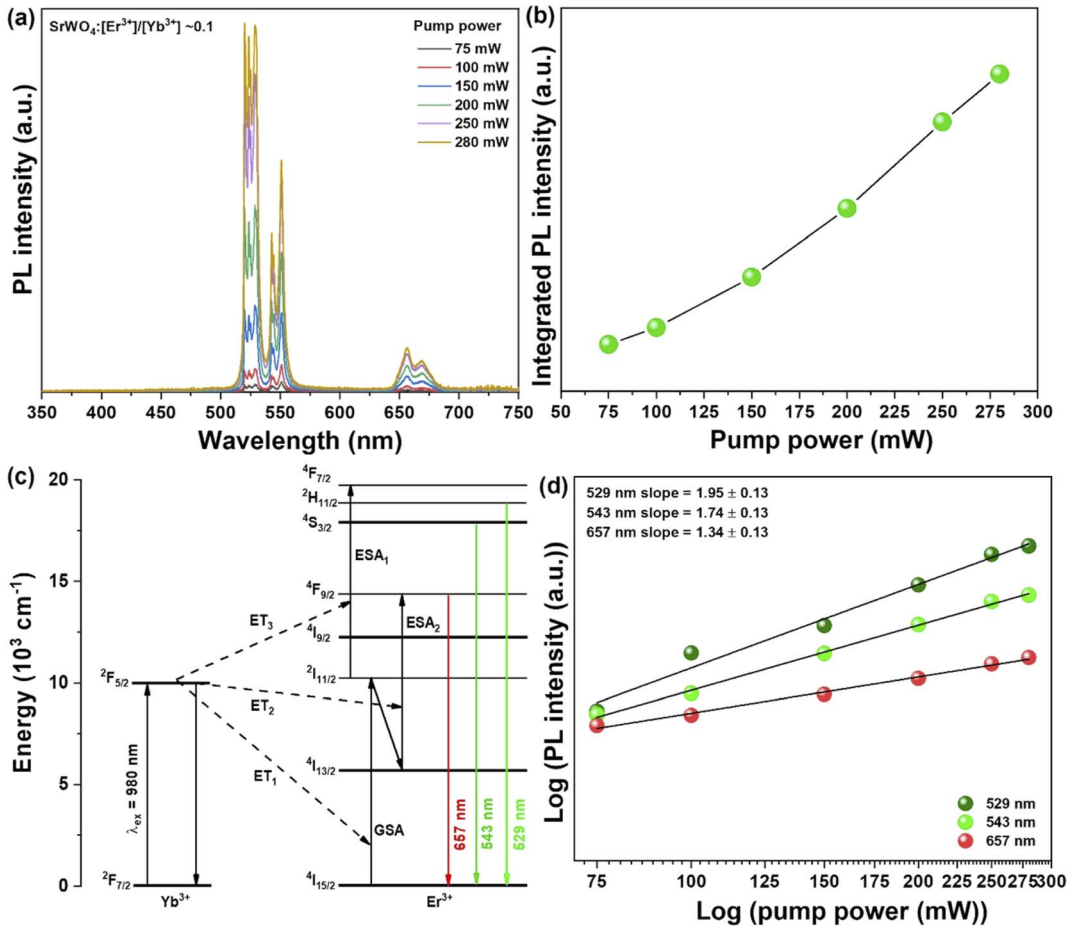

Fig. 5 (a) PL spectra, (b) change in PL intensity, (c) schematic energy transfer process, (d) linear fitting 529 nm, 543 nm, and 657 nm intensity according to pump power under 980 nm of $SrWO_4$:$[Er^{3+}]/[Yb^{3+}] \sim 0.1$ up-conversion phosphors.

where, I is the up-conversion emission intensity, P is the laser power intensity, and n is the number of pumping photons required to excite the upper emitting state. The n is the number of excitation photons involved in the upward conversion process for fluorescence emission, and it can be obtained from the slope of the graph by the logarithm of the pumping light

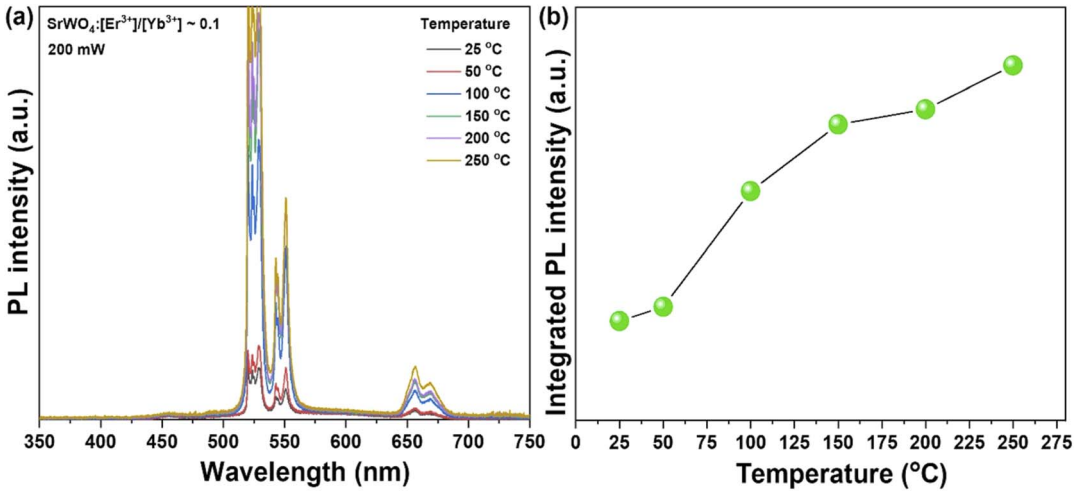

Fig. 6 (a) PL spectra of changing temperature and (b) integrated PL intensity under 980 nm at 200 mW of $SrWO_4$:$[Er^{3+}]/[Yb^{3+}] \sim 0.1$ up-conversion phosphors.

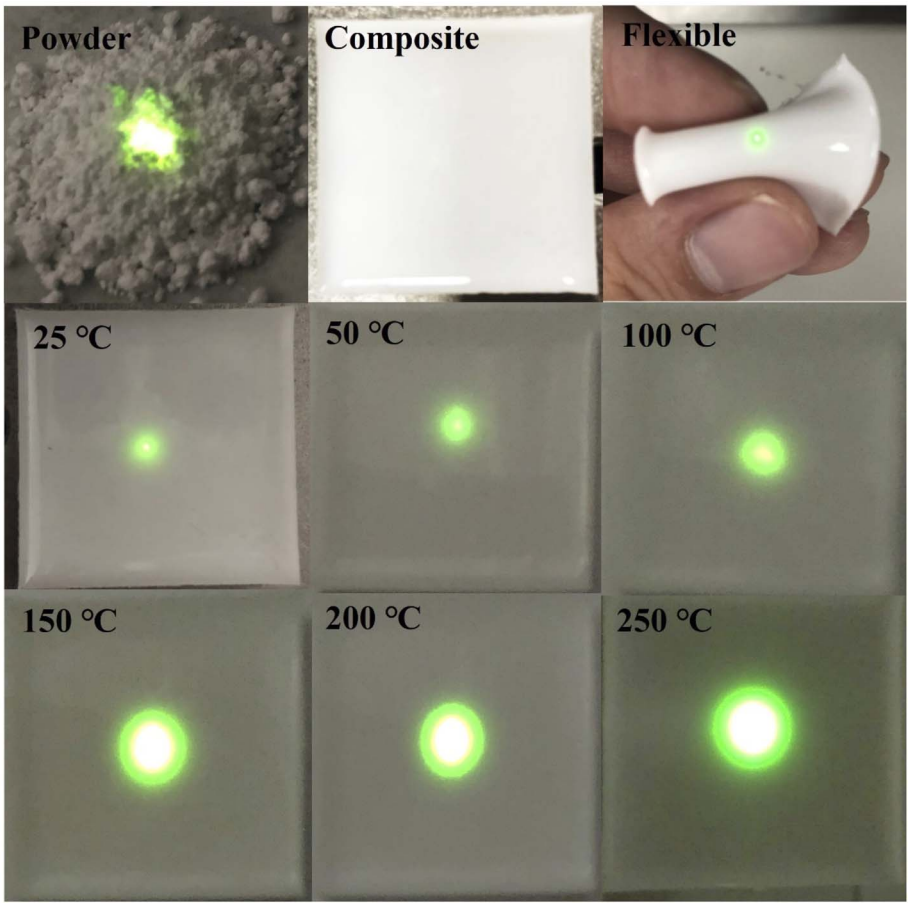

Fig. 7 Photograph of flexible composite under 980 nm at 100 mW, according to the temperature.

intensity and the logarithmic value of the fluorescence intensity. As shown in Fig. 5(d), the slope values of 529 nm (1.95) and 543 nm (1.74) of green emission were greater than 1. This is because the emission of green fluorescence is due to a two-photon process involving two excitation photons. The slope of 657 nm of red fluorescence is 1.34. After the above-mentioned ground state electron absorbs the first photon, it is excited to the $^4I_{11/2}$ level, and then occupies the $^4I_{13/2}$ level by non-radiative transition, and through the ET_2 process. This is a two-photon process that emits red light with a transition of $^4F_{9/2} \rightarrow {}^4I_{15/2}$ by an ESA_2 process that absorbs a second photon.[37,38]

3.3. $SrWO_4$:[Er^{3+}]/[Yb^{3+}] up-conversion phosphors applied for temperature sensing

0.1 g of the synthesized up-conversion $SrWO_4$:[Er^{3+}]/[Yb^{3+}] ~ 0.1 phosphor powder was placed in a copper holder and immersed in a silicone oil bath. The silicone oil bath was placed on a hot plate and the temperature was raised (25–250 °C). After checking the temperature of the powder with an infrared thermometer, a change in luminescence intensity according to temperature change was observed. The spectrum and integrated up-conversion photoluminescence intensity are shown in Fig. 6(a) and (b). In general, it has been reported that the luminescent properties of up-conversion and down-conversion phosphors are reduced due to thermal quenching by external temperature. Ju *et al.* synthesized a down-converted phosphor doped with Sm^{3+} rare earth ions using $SrWO_4$ as a host, and observed a change in luminescence properties by heating it from room temperature to 200 °C. As the temperature increased, the thermal quenching phenomenon was observed very weakly. It was observed that the luminescence intensity rather increased at 190 °C, and it was reported that $SrWO_4$ is an excellent material as a thermally stable host.[39] Liao *et al.* synthesized the $Sc_2(MoO_4)_3$:Yb/Er up-conversion phosphor, and reported the change in luminescence characteristics according to temperature increase, to be negative thermal expansion of the host.[40] This phenomenon is caused by the radiative trapping of Yb^{3+}. This is because lattice shrinkage shortens the distance of Yb^{3+}/Er^{3+} at high temperatures and promotes the radiative trapping of Yb^{3+}. In phosphorescent materials co-doped with Yb^{3+}/Er^{3+}, Yb^{3+} acts not only as a radiation trap to store energy, but also as a sensitizer to transfer energy to Er^{3+}. These radiation traps may promote the release of Er^{3+}. Also, the distance of Yb^{3+}/Er^{3+} becomes shorter as the temperature rises. The ET process between the sensitizer (Yb^{3+}) and the activator (Er^{3+}) is usually thought to be caused by dipole interactions. Its ET efficiency is proportional to r^{-6} (where r is the donor–acceptor distance). Therefore, ET efficiency can be significantly improved

at high temperatures.[40] Desgreniers *et al.* observed changes in Raman signals by giving $CaWO_4$, $SrWO_4$, and $BaWO_4$ changes in temperature (10–300 K) and pressure (910 kbar). As the temperature and pressure increased, no significant change was observed in the high frequency region. However, in the WO_4(Z)–WO_4(Z) stretching region, $CaWO_4$ shifted in phonon energy and frequency due to external environmental factors. However, $SrWO_4$ did not react sensitively, and the frequency shift hardly shifted by about 1–2 cm^{-1}. Using this change, the thermal expansion of the crystal was calculated using the equation below,[41]

$$\frac{d\omega}{dT} = \left(\frac{\partial\omega}{\partial T}\right)_v - \frac{\alpha}{\beta}\left(\frac{\partial\omega}{\partial P}\right)_T \quad (2)$$

where α and β stand for the thermal expansion and isothermal compressibility of the solid. For crystals of $SrWO_4$, the thermal expansion was calculated to be negative. Because the ionic bond between the covalent bonds within the tetrahedron. Furthermore, anomalous temperature behavior for the least energetic stretching vibrations is revealed through negative values and cannot be explained by the hierarchy of bonds theory.[41]

The $SrWO_4$:[Er^{3+}]/[Yb^{3+}] up-conversion phosphor synthesized in this work is also considered to have a stronger luminescence intensity as the temperature increases due to efficient energy transfer between rare earth ions by negative thermal expansion to a thermally stable $SrWO_4$ host. To check whether the synthesized up-conversion phosphor could be used as a temperature sensor, a composite was prepared by mixing PDMS and the phosphor powder. The prepared composite was placed on a hot plate, the temperature was raised, and a 980 nm laser was fixed at 200 mW and irradiated. The temperature was checked with an infrared thermometer on the composite. The produced composite was easily bent by fingers, and it was confirmed that the size of the laser circle reflected on the surface became clearer as the temperature increased, and its size gradually increased. Not only in the powder state, but also in the composite made by mixing with the polymer, the luminescence intensity increased with the rise in temperature. These characteristics suggest the potential for a device that can directly emit a visual danger signal with an increase in temperature (Fig. 7).

4 Conclusion

The precursor was prepared at room temperature by co-precipitation, and crystalline $SrWO_4$ calcined at 800 °C was synthesized. In order to synthesize an up-conversion phosphor material, $SrWO_4$:[Er^{3+}]/[Yb^{3+}] were synthesized using the same experimental procedure, by co-doping with rare earth ions Yb^{3+} and Er^{3+} using $SrWO_4$ as a host. The synthesized powder exhibited a main peak (112) phase in the X-ray diffraction analysis and had a tetragonal structure. Doping with rare earth ions shifted the 2 theta position of the main peak and decreased the lattice constant. With these changes, it was possible to confirm the change in the crystal structure due to the addition of rare earth ions. The surface of the long cylindrical shaped synthesized powder sample was observed by FE-SEM in the longitudinal direction, and particles with a size of about 4 μm were confirmed. When the synthesized phosphor powder was excited with a 200 mW pump power of a 980 nm laser, a strong green spectrum (529 nm, 543 nm) was confirmed. A relatively weak red spectrum at 657 nm was also observed. As the concentration of Er^{3+} ions increased, the luminescence intensity decreased due to the concentration quenching phenomenon. When the intensity of the laser pumping energy was changed, a green fluorescence emission was observed, indicating a two-photon process through an excited state absorption process and an energy transfer process. In addition, the synthesized $SrWO_4$:[Er^{3+}]/[Yb^{3+}] up-conversion phosphor showed an increase in luminescence intensity according to the increase in temperature. The host $SrWO_4$ showed thermal stability due to negative thermal expansion, and energy transfer between Yb^{3+} and Er^{3+} was efficient. It is a phenomenon that has been formed. For application as a temperature sensor, it was confirmed that when a composite was produced by mixing with PDMS and then subjected to a thermal change, as with the powder, the luminescence intensity increased as the temperature increased, so that it could be used as a material for a temperature sensor that could be identified by the naked eye.

Data availability

The data presented in this study are available on request from the corresponding author.

Conflicts of interest

The authors declare no conflict of interest.

Acknowledgements

This research was supported by Basic Science Research Program through the National Research Foundation of Korea (NRF) funded by the Ministry of Education (NRF-2020R1F1A1072676).

References

1 H. J. M. A. A. Zijlmans, J. Bonnet, J. Burton, K. Kardos, T. Vail, R. S. Niedbala and H. J. Tanke, *Anal. Biochem.*, 1999, **267**, 30–36, DOI: 10.1006/abio.1998.2965.
2 A. Rapaport, J. Milliez, M. Bass, A. Cassanho and H. Jenssen, *J. Disp. Technol.*, 2006, **2**, 68–78, DOI: 10.1109/JDT.2005.863781.
3 J. Kundu, Y. Ghosh, A. M. Dennis, H. Htoon and J. A. Hollingsworth, *Nano Lett.*, 2012, **12**, 3031–3037, DOI: 10.1021/nl3008659.
4 B. S. Richards, *Sol. Energy Mater. Sol. Cells*, 2006, **90**, 1189–1207, DOI: 10.1016/j.solmat.2005.07.001.
5 G. Blasse and A. Bril, *J. Chem. Phys.*, 1967, **47**, 5139–5145, DOI: 10.1063/1.1701771.
6 S. Adachi, *J. Lumin.*, 2018, **202**, 263–281, DOI: 10.1016/j.jlumin.2018.05.053.
7 Y. Zhou, Y. Cheng, Q. Huang, J. Xu, H. Lin and Y. Wang, *J. Mater. Chem. C*, 2021, **9**, 222–223, DOI: 10.1039/d0tc05759b.

8 J. H. Zeng, T. Xie, Z. H. Li and Y. Li, *Cryst. Growth Des.*, 2007, 7, 2774–2777, DOI: 10.1021/cg070477n.
9 V. Vaiano, O. Sacco, G. Iervolino, D. Sannino, P. Ciambelli, R. Liguori, E. Bezzeccheri and A. Rubino, *Appl. Catal., B*, 2015, **176–177**, 594–600, DOI: 10.1016/j.apcatb.2015.04.049.
10 B. Qu, Y. Jiao, S. He, Y. Zhu, P. Liu, J. Sun, J. Lu and X. Zhang, *J. Alloys Compd.*, 2016, **658**, 848–853, DOI: 10.1016/j.jallcom.2015.11.024.
11 A. Shalav, B. S. Richards and M. A. Green, *Sol. Energy Mater. Sol. Cells*, 2007, **91**, 829–842, DOI: 10.1016/j.solmat.2007.02.007.
12 A. M. Darwish, S. Moore, A. Mohammad, D. Alexander, T. Bastian, W. Dorlus, S. Sarkisov, D. Patel, P. Mele, B. Koplitz and D. Hui, *Composites, Part B*, 2017, **109**, 82–90, DOI: 10.1016/j.compositesb.2016.10.053.
13 A. M. Darwish, S. Wilson, A. Balckwell, K. Taylor, S. S. Sarkisov, D. N. Patel and B. Koplitz, *Ammonia Sensor Based on Polymer-Inorganic Nano-Composite Thin Film Upconversion Light Emitter Prepared by Double-Beam Pulsed Laser Deposition*, 2015.
14 L. D. Carlos, R. A. S. Ferreia, V. Z. Bermudez, B. Julian-Lopez and P. Escribano, *Chem. Soc. Rev.*, 2011, **40**, 536–549, DOI: 10.1039/c0cs00069h.
15 K. Pavani, J. Suresh Kumar, K. Srikanth, M. J. Soares, E. Pereira, A. J. Neves and M. P. F. Graça, *Sci. Rep.*, 2017, **7**, 1–15, DOI: 10.1038/s41598-017-17725-z.
16 C. S. Lim, *Trans. Electr. Electron. Mater.*, 2018, **20**, 60–66, DOI: 10.1007/s42341-018-0083-z.
17 T. Deng, S. Yan, X. Jiang and Q. Zhang, *Int. J. Opt.*, 2019, **2019**, 1–6, DOI: 10.1155/2019/4814793.
18 E. W. Barrera, Q. Madueño, F. J. Novegil, A. Speghini and M. Bettinelli, *Opt. Mater.*, 2018, **84**, 354–359, DOI: 10.1016/j.optmat.2018.07.022.
19 A. Pandey, V. K. Rai, R. Dey and K. Kumar, *Mater. Chem. Phys.*, 2013, **139**, 483–488, DOI: 10.1016/j.matchemphys.2013.01.043.
20 J. Jung, J. Kim, Y. Shim, D. Hwang and C. S. Son, *Materials*, 2020, **13**, 4165, DOI: 10.3390/ma13184165.
21 J. Jung, S. Yi, D. Hwang and C. Son, *Materials*, 2021, **14**, 3717, DOI: 10.3390/ma14133717.
22 J. Ruan, T. Yuan, Y. Pang, S. Luo, C. Peng, J. Yang and S. Zheng, *Carbon*, 2018, **126**, 9–16, DOI: 10.1016/j.carbon.2017.09.099.
23 P. P. Ortega, B. Hangai, H. Moreno, L. S. R. Rocha, M. A. Ramírez, M. A. Ponce, E. Longo and A. Z. Simões, *J. Alloys Compd.*, 2021, **888**, 161517, DOI: 10.1016/j.jallcom.2021.161517.
24 X. Wang, Y. Wang, Y. Bu, X. Yan, J. Wang, P. Cai, T. Vu and H. J. Seo, *Sci. Rep.*, 2017, **7**, 43383, DOI: 10.1038/srep43383.
25 R. D. Shannon, *Acta Crystallogr., Sect. A: Found. Adv.*, 1976, **32**, 751–767, DOI: 10.1107/S0567739476001551.
26 E. Ryu and Y. Huh, *Mater. Lett.*, 2008, **62**, 3081–3083, DOI: 10.1016/j.matlet.2008.01.108.
27 Y. Hu, X. Liang, Y. Wang, E. Liu, X. Hu and J. Fan, *Ceram. Int.*, 2015, **41**, 14545–14553, DOI: 10.1016/j.ceramint.2015.07.171.
28 J. Zhao, Y. Sun, X. Kong, L. Tian, Y. Wang, L. Tu, J. Zhao and H. Zhang, *J. Phys. Chem. B*, 2008, **112**, 15666–15672, DOI: 10.1021/jp805567k.
29 W. A. Pisarski, L. Grobelny, J. Pisarska, R. Lisiecki and W. Ryba-Romanowski, *J. Alloys Compd.*, 2011, **509**, 8088–8092, DOI: 10.1016/j.jallcom.2011.05.056.
30 B. Wei, L. Z. Zhang, Z. B. Lin and G. F. Wang, *Mater. Res. Innovations*, 2007, **11**, 154–157, DOI: 10.1179/143307507X225605.
31 G. Xiang, X. Liu, W. Liu, B. Wang, Z. Liu, S. Jiang, X. Zhou, L. Li, Y. Jin and J. Zhang, *J. Am. Ceram. Soc.*, 2020, **103**, 2540–2547, DOI: 10.1111/jace.16939.
32 M. Erdem and B. Sitt, *Opt. Mater.*, 2015, **46**, 260–264, DOI: 10.1016/j.optmat.2015.04.029.
33 G. A. Fernández-Alcober and P. Shumyatsky, *J. Algebra*, 2018, **500**, 19–29, DOI: 10.1016/j.jalgebra.2016.07.041.
34 G. Bilir, A. Kaya, H. Cinkaya and G. Eryürek, *Spectrochim. Acta, Part A*, 2016, **165**, 183–190, DOI: 10.1016/j.saa.2016.04.042.
35 P. Woźny, M. Runowski and S. Lis, *J. Lumin.*, 2019, **209**, 321–327, DOI: 10.1016/j.jlumin.2019.02.008.
36 M. Guan, H. Zheng, L. Mei, M. S. Molokeev, J. Xie, T. Yang, X. Wu, S. Huang and Z. Huang, *J. Am. Ceram. Soc.*, 2015, **98**, 1182–1187, DOI: 10.1111/jace.13415.
37 M. A. Chamarro and R. Cases, *Infrared to visible upconversion of Er^{3+} ions in Yb^{3+} doped fluorohafnate glasses*, Elsevier BV, 1990.
38 X. Xia, A. Volpi, J. Y. D. Roh, M. C. De Siena, D. R. Gamelin, M. P. Hehlen and P. J. Pauzauskie, *J. Lumin.*, 2021, **236**, 118006, DOI: 10.1016/j.jlumin.2021.118006.
39 Z. JU, R. WEI, J. MA, C. PANG and W. LIU, *J. Alloys Compd.*, 2010, **507**, 133–136, DOI: 10.1016/j.jallcom.2010.07.138.
40 J. Liao, M. Wang, F. Lin, Z. Han, B. Fu, D. Tu, X. Chen, B. Qiu and H. Wen, *Nat. Commun.*, 2022, **13**, 2090, DOI: 10.1038/s41467-022-29784-6.
41 S. Desgreniers, S. Jandl and C. Carlone, *J. Phys. Chem. Solids*, 1984, **45**, 1105–1109, DOI: 10.1016/0022-3697(84)90004-0.